Study of the laminas' stress-strain state for cross-ply composites with the $[\pm 45°]_{2s}$ lay-up: tensile tests

V. Paimushin[1,2*], *V.* Firsov[1], and *R.* Gazizullin[1]

[1]Kazan National Research Technical University named after A. N. Tupolev – KAI, 10, K.Marx St., 420111 Kazan, Russia
[2] Kazan Federal University, 18, st. Kremlyevskaya, 420008 Kazan, Russia

Abstracts. In this paper we have analysed the relations that allows one to determine the components of strains and stresses in the orthotropic axes of layered fiber reinforced composite materials in tensile and compression experiments for test specimens with the $[\pm 45°]_{2s}$ lay-up. In particular, such relations were compiled on the assumption that in a cross-ply fiber composite two adjacent layers with the $[\pm\varphi]$ lay-ups can be considered as one symmetrically reinforced layer with orthotropic properties. To establish the degree of accuracy of these relationships and assumptions, numerical experiments were carried out to determine the parameters of the stress-strain state of specimens consisting of two and four monolayers of a unidirectional fibrous composite material with the $[\pm 45°]_{2s}$ lay-up. The analysis has been performed in the ANSYS finite element analysis program system in a linear formulation of two- and three-dimensional problems. It is shown that in the central zone of the specimen, the theoretical-experimental methodology based on the above mentioned relations has a sufficient degree of accuracy. Based on the analysis of results of three-dimensional problems, the formation of a linear torque in the specimen, which causes the twisting of some zones of the specimen along its length, has been revealed.

1 Introduction

In mechanics of deformable solids there is a direction of research related to formulation and solution of problems about internal and surface (peripheral) forms of stability loss of layered fibrous composites reinforced by straight or curvilinear fibers under certain loading conditions. Such problems are important because in the construction of the strength theories of composite materials the loss of stability of the composite structure is taken as a possible failure mechanism. A great cycle of research in this direction was carried out in the second half of the last century, the results of which were given in many scientific articles and monographs [1-3, etc.]. The works [4-10] devoted to experimental and theoretical study of failure mechanisms of fiber composites during tests of specimens in accordance with the developed standards should be referred to the same direction of research. For a more detailed study of the possibility of various internal buckling forms realization for elements made of a

*Corresponding author: vpajmushin@mail.ru

unidirectional fiber composite in the case of tension of test specimens with the $[\pm 45°]_{2s}$ lay-up, in addition to studies [11, 12], at the first stage it is advisable to carry out a numerical study of the stresses and strains formed in such structures.

2 Relationships for determining the components of stresses and strains for layered fiber reinforced composites in the orthotropy axes

In accordance with the ASTM D3518 test standard [13], tensile and compression tests of specimens with the $[\pm 45°]_{2s}$ lay-up and an even number of laminas $2s$ (considerable to exclude the specimens bending in the direction of the axis y (Fig. 1)) are performed to determine the shear modulus G_{12} in the orthotropic axes of a single lamina x_1, x_2.

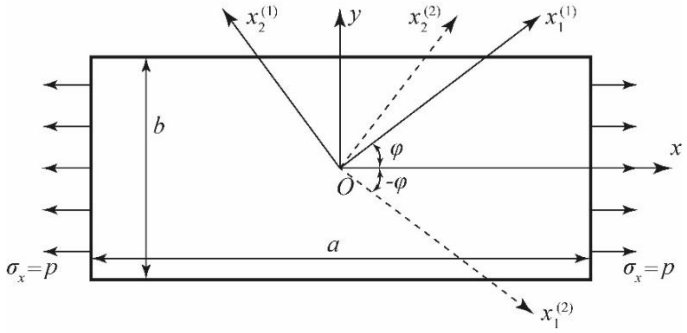

Fig. 1. Scheme of reinforcement in the first two laminas of a test specimen made of fiber reinforced composite with the $\left[\pm\varphi\right]_{2s}$ lay-up under tension stress $\sigma_x = p$.

The result of such specimens' tests, represented in the form of a flat elongated rod, under single tension is always a physically non-linear stress-strain curve up to failure. This curve gives the $\sigma_x = \sigma_x\left(\varepsilon_x\right)$ dependence between the normal stress $\sigma_x = p$ averaged over the $x = const$ cross-sectional area and the corresponding axial strain ε_x measured in the x axial direction in the vicinity of the central point 0 (Fig. 1), Poisson's ratio $\nu_{xy} = -\varepsilon_y \big/ \varepsilon_x$, and the failure stress σ_x^{+*}. Based on such a stress-strain curve of the specimen, the relationship between the secant modulus of elasticity $\hat{E}_x$ and the axial deformation ε_x in the axes of the specimen can be established. Using the relations derived in [11, 14], of the following form

$$\sigma_{12} = \frac{\sigma_x}{2}, \qquad \gamma_{12} = \frac{2\left(1+\nu_{xy}\right)}{2+\varepsilon_x\left(1-\nu_{xy}\right)}\varepsilon_x \approx \left(1+\nu_{xy}\right)\varepsilon_x, \tag{1}$$

we construct a shear strain curve $\sigma_{12} = \sigma_{12}\left(\gamma_{12}\right)$. This curve gives the dependence between the shear stress σ_{12} and the corresponding shear strain γ_{12} in the orthotropic axis

x_1, x_2. Using the $\sigma_{12} = \sigma_{12}\left(\gamma_{12}\right)$ curve, we can also construct the dependence $\hat{G}_{12} = \hat{G}_{12}\left(\gamma_{12}\right)$ between the secant shear modulus and the shear strain γ_{12}.

It should be noted that in tensile tests of specimens with $[0°]_s$ and $[90°]_s$ lay-ups (s is the number of lamina in the specimen) with fibers located along and across to the direction of the acting load the mechanical characteristics of a single monolayer of fiber reinforced composite in its orthotropy axis x_1, x_2 have been determined earlier. The corresponding stress-strain curve for a unidirectional CFRP can be considered linear up to the failure of the specimens [15, 16]. This fact makes it possible to determine elastic moduli E_1 (in the direction of the fibers), E_2 (in the direction across the fibers) and Poisson's ratio ν_{21} for a lamina of composite from test results. Then it is possible to calculate another Poisson's ratio ν_{12} from the dependence $E_1\nu_{12} = E_2\nu_{21}$.

For a single k-th lamina of composite laid at an φ angle to the specimen axis (Fig. 1) the physical relations in the specimen axes are represented as

$$\begin{aligned} &\sigma_x^{(k)} = A_{11}\varepsilon_x^{(k)} + A_{12}\varepsilon_y^{(k)} \pm A_{13}\gamma_{xy}^{(k)},\ \sigma_y^{(k)} = A_{12}\varepsilon_x^{(k)} + A_{22}\varepsilon_y^{(k)} \pm A_{13}\gamma_{xy}^{(k)}, \\ &\sigma_{xy}^{(k)} = \pm A_{13}\varepsilon_x^{(k)} \pm A_{23}\varepsilon_y^{(k)} + A_{33}\gamma_{xy}^{(k)}, \end{aligned} \tag{2}$$

here sign "-" refers to the lamina with the $k+1$ number, laid at an angle $-\varphi$. The coefficients in (2) are determined by the following formulas

$$\begin{aligned} &A_{11} = A_{22} = C + \hat{G}_{12},\ A_{12} = C - \hat{G}_{12},\ C = \frac{E_1^* + E_2^*}{4} + \frac{E_1^*\nu_{12}}{2}, \\ &A_{13} = A_{23} = \frac{E_1^* - E_2^*}{4},\ A_{33} = \frac{E_1^* + E_2^*}{4} - \frac{E_1^*\nu_{12}}{2}. \end{aligned} \tag{3}$$

In composite mechanics [17], two adjacent lamina laid at $\pm\varphi$ angles are considered as one symmetrically reinforced layer with orthotropic properties.

Physical relations for such a layer with the introduction of averaged stresses

$$\begin{aligned} &\sigma_x = \langle\sigma_x\rangle = \left(\sigma_x^{(1)} + \sigma_x^{(2)}\right)\Big/2,\ \sigma_y = \langle\sigma_y\rangle = \left(\sigma_y^{(1)} + \sigma_y^{(2)}\right)\Big/2, \\ &\sigma_{xy} = \langle\sigma_{xy}\rangle = \left(\sigma_{xy}^{(1)} + \sigma_{xy}^{(2)}\right)\Big/2 \end{aligned} \tag{4}$$

and strains

$$\begin{aligned} &\varepsilon_x = \langle\varepsilon_x\rangle = \left(\varepsilon_x^{(1)} + \varepsilon_x^{(2)}\right)\Big/2,\ \varepsilon_y = \langle\varepsilon_y\rangle = \left(\varepsilon_y^{(1)} + \varepsilon_y^{(2)}\right)\Big/2, \\ &\gamma_{xy} = \langle\gamma_{xy}\rangle = \left(\gamma_{xy}^{(1)} + \gamma_{xy}^{(2)}\right)\Big/2 \end{aligned} \tag{5}$$

follow from (2),(4),(5) and have the following form

$$\sigma_x = A_{11}\left(\varepsilon_x + \nu_{yx}\varepsilon_y\right),\ \sigma_y = A_{22}\left(\nu_{xy}\varepsilon_x + \varepsilon_y\right),\ \sigma_{xy} = A_{33}\gamma_{xy}, \tag{6}$$

here $\nu_{yx} = A_{12}/A_{11}$, $\nu_{xy} = A_{12}/A_{22}$. Note that these expressions are based on the assumption $A_{11} \neq A_{22}$, $\nu_{xy} \neq \nu_{yx}$, but $A_{11}\nu_{yx} = A_{22}\nu_{xy}$.

Along with the stresses (4) and strains (5) averaged over the thickness of two adjacent layers, we introduce into consideration stresses and strains

$$\begin{aligned}
&\sigma_x^- = \frac{\sigma_x^{(1)} - \sigma_x^{(2)}}{2},\ \sigma_y^- = \frac{\sigma_y^{(1)} - \sigma_y^{(2)}}{2},\ \sigma_{xy}^- = \frac{\sigma_{xy}^{(1)} - \sigma_{xy}^{(2)}}{2},\\
&\varepsilon_x^- = \frac{\varepsilon_x^{(1)} - \varepsilon_x^{(2)}}{2},\ \varepsilon_y^- = \frac{\varepsilon_y^{(1)} - \varepsilon_y^{(2)}}{2},\ \gamma_{xy}^- = \frac{\gamma_{xy}^{(1)} - \gamma_{xy}^{(2)}}{2},
\end{aligned} \tag{7}$$

which, under the assumptions $A_{11} \neq A_{22}$, $\nu_{xy} \neq \nu_{yx}$, lead to the relations

$$\begin{aligned}
&\sigma_x = A_{11}\varepsilon_x + A_{12}\varepsilon_y + A_{13}\gamma_{xy}^-,\ \sigma_y = A_{12}\varepsilon_x + A_{22}\varepsilon_y + A_{23}\gamma_{xy}^-,\\
&\sigma_{xy} = A_{13}\varepsilon_x^- + A_{23}\varepsilon_y^- + A_{33}\gamma_{xy},
\end{aligned} \tag{8}$$

$$\begin{aligned}
&\sigma_x^- = A_{11}\varepsilon_x^- + A_{12}\varepsilon_y^- + A_{13}\gamma_{xy},\ \sigma_y^- = A_{12}\varepsilon_x^- + A_{22}\varepsilon_y^- + A_{23}\gamma_{xy},\\
&\sigma_{xy}^- = A_{13}\varepsilon_x + A_{23}\varepsilon_y + A_{33}\gamma_{xy}^-.
\end{aligned} \tag{9}$$

Formulated relations (8) can be reduced to relations (6) only under the introduction of assumptions $\varepsilon_x^- = \varepsilon_y^- = \gamma_{xy}^- = 0$, due to which relations (9) take the form

$$\sigma_x^- = A_{13}\gamma_{xy},\ \sigma_y^- = A_{23}\gamma_{xy},\ \sigma_{xy}^- = A_{13}\varepsilon_x + A_{23}\varepsilon_y. \tag{10}$$

Note that when the specimen with the $[\pm 45°]_{2s}$ lay-up is tensioned by stress p, the following equalities take place

$$\sigma_x = p,\ \sigma_y = 0,\ \gamma_{xy} = 0,\ \varepsilon_y^{(k)} = \varepsilon_y = -\nu_{xy}\varepsilon_x. \tag{11}$$

Due to the symmetry about the $0x$ axis of the strain components of the layers, the following relations are valid

$$\varepsilon_{11}^{(1)} = \varepsilon_{11}^{(2)} = \varepsilon_{22}^{(1)} = \varepsilon_{22}^{(2)} = \varepsilon_{11}. \tag{12}$$

To establish the degree of accuracy of relations (6), (11), (12) and assumptions $\varepsilon_x^- = \varepsilon_y^- = \gamma_{xy}^- = 0$, special studies are required. A detailed numerical analysis of the stress-strain state formed in test specimens with the $[\pm 45°]_{2s}$ lay-up under tension (compression) can be carried out, in particular, on the basis of well-known numerical methods using commercial software packages.

3 Results of numerical research

It should be noted that in the manufacture of structural elements from fibrous composite materials a heterogeneity over the thickness always formed in the structure of their layers. This heterogeneity consists in the alternation of rigid monolayers (including composite fibers) with less rigid layers of pure binder. For example, as shown by the analysis of the structure of composite material made of ELUR-P carbon fiber and the XT-118 epoxy binder carried out using a Carl Zeiss Stemi 2000 optical microscope, the thickness of the specified binder layer (hereinafter called to as adhesive) is about 0.07 mm, while the thickness of a rigid monolayer is about 0.12 mm. While the rigid monolayer has an elastic modulus in the fiber direction of about 100 GPa, the adhesion layer of composite material, which can be considered isotropic and linearly elastic up to failure [15] has an elastic modulus of about 3 GPa at a Poisson's ratio of 0.34. In this regard, the adhesive layers of composite material can be classified as transversely soft (in accordance with the terminology of [2]) in comparison with rigid monolayers.

In connection with the above mentioned, a numerical study of the stress-strain state formed in tension of test specimens having a length of $a = 110$ mm and a width of $b = 25$ mm (Fig. 1) and made of the above described composite material with $[\pm 45°]_2$ (two-layer specimen) and $[\pm 45°]_4$ (four-layer specimen) lay-ups has been performed in the finite-element ANSYS software package. It is important to note that, in contrast to [12], in calculations it has been assumed that between the rigid layers with a thickness of 0.12mm there are adhesion layers of binder with a thickness of 0.07mm. The calculations were carried out for specimens with effective elastic characteristics of rigid layers' materials equal to $E_1 = 105$ GPa (in the fiber direction), $E_3 = E_2 = 5.7$ GPa (in the cross fiber direction), $\nu_{12} = \nu_{13} = \nu_{23} = 0.34$ and $G_{12} = G_{13} = G_{23} = 3.2$ GPa. The material of adhesion layers was taken isotropic with elastic characteristics equal to $E = 2.5$ GPa, $\nu = 0.3$. The tensile modeling of test specimens under kinematic loading conditions was carried out by specifying the displacement of the edge $x = a/2$ in the direction of the x axis by a value of $u = 0.01a$ with a fixed edge $x = -a/2$. The analysis was performed by modeling each layer of the specimen with three-dimensional SOLID186 elements with one element through the thickness of each of the layers. The results obtained were compared to the results of a planar problem statement using a two-dimensional PLANE183 element (assuming that the plate is in a plane stressed state) with the values of stiffness coefficients averaged over the thickness of the layer package. Their values in the specimen axes $x0y$ were calculated by formulas (3).

For illustration purposes, Figs. 2 and 3 show graphs of normal stresses σ_x and tangential stresses σ_{xy} changing along the coordinate y in different sections of the test specimens. Here, solid and dashed lines indicate curves corresponding to parameters of stress-strain state on the front surfaces of the first and the last layers of the test specimen, respectively, obtained on the basis of a three-dimensional formulation of the problem, and the dash-dot line indicate curves corresponding to the results obtained on the basis of the plane statement of the problem. Letters a and c denote the graphs of the corresponding parameters' distribution in the specimens with the $[\pm 45°]_2$ lay-up in sections $x = 0$ and $x = -a/4$, respectively, and letters b and d denote the graphs in the specimens with the $[\pm 45°]_4$ lay-up in the same sections.

Analyzing the obtained results, the presence of pronounced boundary effects near the corner points was revealed. Furthermore one can see a small variability of the stress components in the central zone of the specimen. Far from the center of the samples (in the

sections $x=-a/4$), a slight asymmetry of the stress values in the layer relative to the x axis can be also revealed. It should be noted that in Figs. 2 and 3 the curve for the N -th layer may completely coincide with the curve for the first layer, and therefore be absent from the graph. Also note that the corresponding dependences of the normal stresses σ_y turned out to be orders of magnitude smaller than the normal stresses σ_x.

As it follows from Fig. 3, tangential stresses σ_{xy} in rigid layers with opposite lay-up angles have different signs. Because there is a certain distance between the layers, at such a stress-strain state in the cross section $x=const$ of the specimen a torsional moment is formed. This torsional moment twists some zones of the specimen. In order to illustrate this phenomenon, Fig. 4 shows graphs of the change in the deflection w of the specimen mid-surface in three different cross-sections. Fig. 4a illustrate graphs for a specimen consisting of two layers, and Fig. 4b illustrate graphs for a specimen consisting of four layers. In these figures, the solid lines correspond to the deflections of the middle surface in the section $x=-a/4$, the dashed lines in the section $x=a/4$, and the dash-dotted lines in the section $x=0$.

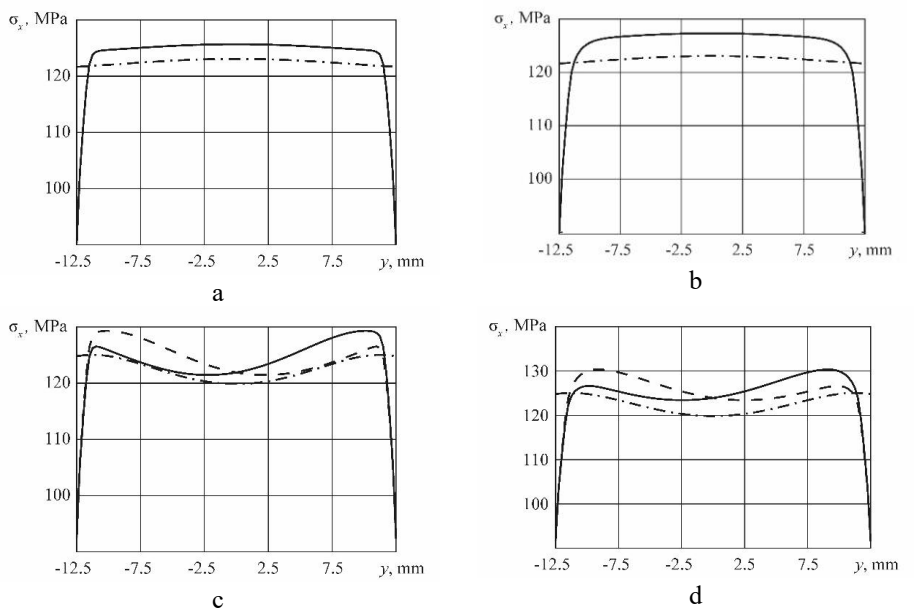

Fig. 2. Diagrams of normal stresses σ_x changing along the coordinate y in sections $x=0$ and $x=-a/4$.

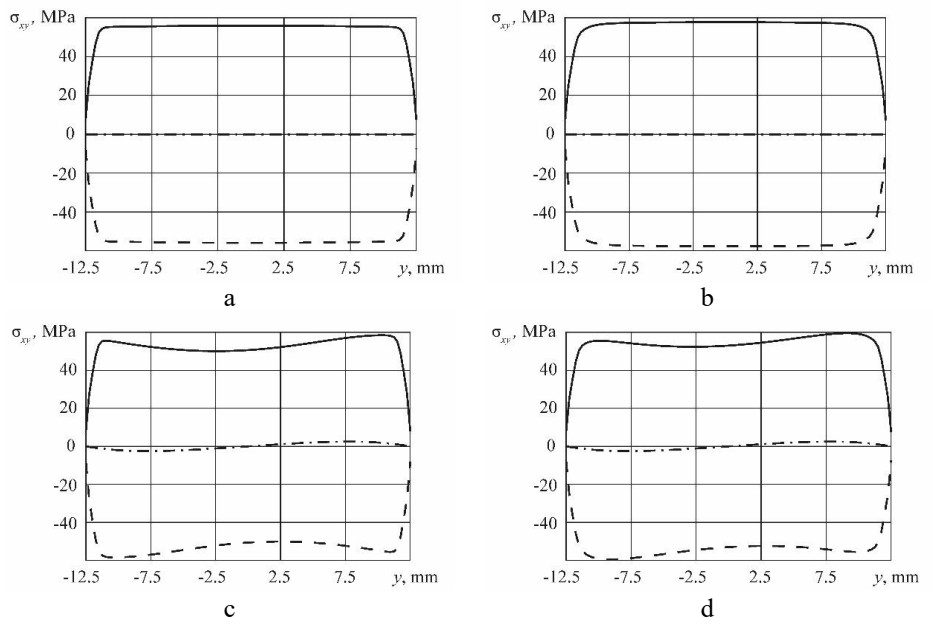

Fig. 3. Diagrams of tangential stresses σ_{xy} changing along the coordinate y in sections $x = 0$ and $x = -a/4$.

These figures show a very significant deflection of the middle surface of the two-layer specimen in the areas one-quarter of the length away from the center. In the four-layer specimen, the deflection of the median plane was also detected in similar areas, but their values were an order of magnitude smaller. This phenomenon can be explained by the fact that the inner and outer pairs of layers form torsional moments of opposite signs, which partially compensate each other. Furthermore the torsional stiffness of the four-layer specimen is much greater in comparison with the two-layer specimen. It is important to note that the results described above cannot be obtained on the basis of the equations using relations (6), as well as in a two-dimensional formulation of the problem with averaging over the thickness of the stiffness properties of the layer's material. This implies a fundamentally important conclusion that the most accurate and meaningful description of deformation mechanics of composite plates with cross-reinforced monolayers is possible only on the basis of refined equations. This is especially important for structures with only two layers.

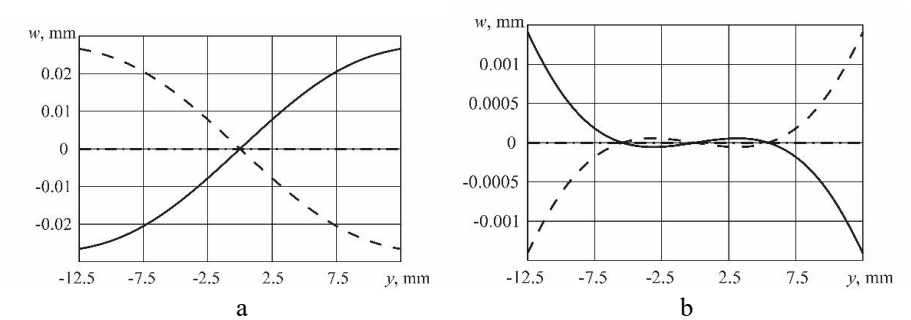

Fig. 4. Diagrams of the change in the deflection w of the specimen mid-surface along the coordinate y in sections $x = -a/4$, $x = a/4$ and $x = 0$.

4 Conclusion

In conclusion, it should be added that the obtained results allow us to evaluate the accuracy degree of the experimental method stated in the theoretical part. In particular, the analysis of linear strains ε_x, Poisson's ratio ν_{xy} and shear strains γ_{12} allow us to estimate the reliability of the second formula in (1). Calculations have shown that this dependence is fulfilled with an error of less than 0.01% along the entire length of the specimen. The only exceptions are in the corner points, and only in the case of a flat formulation of the problem. The error in this case can reach the order of 10%. Hence, a conclusion can be formulated that the theoretical-experimental method for constructing the $\hat{G}_{12} = \hat{G}_{12}(\gamma_{12})$ dependence stated in [18, 19] and based on formulas (1), (3), relations (6) and (11) has a sufficient degree of accuracy in the central zone of the specimen with $[\pm 45°]_2$ lay-up at $s \geq 2$.

Acknowledgement

This paper has been supported by the Russian Science Foundation (Project No. 19–19–00059) (Sect. 1,2) and by the Kazan Federal University Strategic Academic Leadership Program ("PRIORITY-2030") (Sect. 3-4).

References

1. A.N. Guz, *Stability of elastic bodies under finite deformations* (Naukova Dumka Kiev, 1973)
2. V.V. Bolotin, Yu.N. Novichkov, *Mechanics of multilayer structures* (Mechanical Engineering, Moscow, 1980)
3. B.W. Rosen, Proceedings of the American Society of metals, 574-586 (1965)
4. B. Budiansky, N.A. Fleck, J. Mech. Phys. Solids **41(1)**, 183-211 (1993)
5. Li Xu Yong, K.L. Reifsnider, J. Compos. Mater. **27(6)**, 572-588 (1993)
6. G. Zhang, R.A. Latour, J. Thermoplast. Compos. Mater. **6(4)**, 298-311 (1993)
7. G. Zhang, R.A. Latour, Compos. Sci. Technol. **51(1)**, 95-109 (1994)
8. N.K. Naik, R.S. Kumar, Compos. Struct. **46(3)**, 299-308 (1999)
9. A. Jumahat, C. Soutis, F.R. Jones, A. Hodzic, Compos. Struct. **92(2)**, 295-305 (2010)
10. V.N. Paimushin, S.A. Kholmogorov, R.K. Gazizullin, Mech. Compos. Mater. **53(6)**, 737-752 (2017)
11. V.N. Paimushin, N.V. Polyakova, S.A. Kholmogorov, M.A. Shishov, Mech. Compos. Mater. **54(2)**, 133-144 (2018)
12. V.N. Paimushin, R.A. Kaymov, V.A. Firsov et al, Uchenye Zapiski Kazanskogo Universiteta. Seriya Fiziko-Matematicheskie Nauki **161(1)**, 86-109 (2019)
13. *D3518/3518M-94. Standard Test Method for In-Plane Shear Response of Polymer Matrix Composite Materials by Tensile Test of a ±45° Laminate, vol. 15.03, Space Simulation; Aerospace and Aircraft; Composite Materials* (ASTM International, West Conshohocken, PA, 2005)
14. V.N. Paimushin, R.K. Gazizullin, M.A. Shishov, J. Appl. Mech. Tech. Phys. **60(3)**, 548-559 (2019)
15. V.N. Paimushin, S.A. Kholmogorov, Mech. Compos. Mater. **54(1)**, 2-12 (2018)

16. R.A. Kayumov, S.A. Lukankin, V.N. Paimushin, S.A. Kholmogorov, Uchenye Zapiski Kazanskogo Universiteta. Seriya Fiziko-Matematicheskie Nauki **157(4)**, 112-132 (2015)
17. V.V. Vasiliev, *Mechanics of structures made of composite materials* (Mashinostroenie, Moscow, 1988)
18. V.N. Paimushin, S.A. Kholmogorov, M.V. Makarov et al, Angew. Math. Mech. **99(1)**, e201800063 (2019)
19. V.N. Paimushin, D.V. Tarlakovskii, S.A. Kholmogorov, Uchenye Zapiski Kazanskogo Universiteta. Seriya Fiziko-Matematicheskie Nauki **158(3)**, 350-375 (2016)
20. V.N. Paimushin, R.K. Gazizullin, M.A. Shishov, Mech. Compos. Mater. **55(6)**, 743-760 (2020)